MULTI-DIMENSIONAL BIOMEDICAL IMAGE DE-NOISING USING HAAR TRANSFORM

Eva Hostalkova, Oldrich Vysata, Ales Prochazka

Institute of Chemical Technology in Prague, Department of Computing and Control Engineering
Technicka Street 5, 166 28 Prague 6, Czech Republic
Email: Eva.Hostalkova@vscht.cz, Vysata@neurol.cz, A.Prochazka@ieee.org
Phone: +420 220 444 198, Web: dsp.vscht.cz

ABSTRACT

Image de-noising and enhancement form two fundamental problems in many engineering and biomedical applications. The paper is devoted to the study of the multi-resolution approach to this topic employing the Haar wavelet transform and its application to processing of volumetric magnetic resonance image sets corrupted with additional noise. The resulting coefficients are thresholded and exploited for subsequent reconstruction. The Haar transform is evaluated using both the two-dimensional approach applied individually to each image layer, and the three-dimensional technique performed on the image volume as a whole. In noise reduction, the latter approach profits from similarities between the neighbouring image layers and shows a considerable improvement over the former method. Results are presented in numerical and graphical forms using three-dimensional visualization tools.

Index Terms— Wavelet transform, image decomposition and reconstruction, Haar transform, de-noising, biomedical image processing

1. INTRODUCTION

Fundamental problems encountered in digital processing of both one-dimensional and multi-dimensional signals include rejection of their undesirable parts [1, 2], feature extraction, classification and restoration of their missing or corrupted components. Multi-resolution approach related to wavelet transform [3, 4, 5] is used in many cases to simplify these processes and to improve their robustness. Image resolution enhancement [6, 7] and volumetric reconstruction [8, 9] form further problems related to these topics.

Biomedical image processing represents an extensive area based upon theoretical principles of multi-dimensional processing methods. Related problems include multirate analysis, processing and coding of biomedical images [10, 11].

The paper is devoted to the use of the wavelet transform and multi-resolution decomposition of biomedical image volumes to improve results of the de-noising process applied separately to each image layer of the body. In the initial part of the paper, the Haar transform computation algorithm is proposed starting with 1-D signal and proceeding to 2-D images and 3-D image sets.

Thanks to Research grant No. MSM 6046137306

The proposed method is applied to multi-layer magnetic resonance (MR) biomedical images. An example of the biomedical structures studied further is presented in Fig. 1. After noise addition, these multi-layer images are processed by both 2-D and 3-D Haar transform involving the coefficients thresholding procedure. This approach is closely related to many possibilities of the use of wavelet transform in magnetic resonance imaging studied by many authors [12, 13].

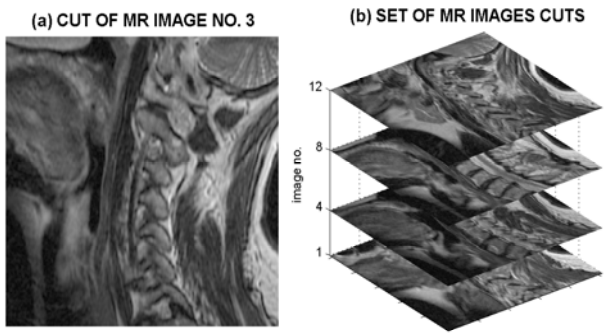

Fig. 1. Real data standing for **(a)** a selected spinal MR image and **(b)** four chosen slices of the MR data set (number 3]

2. HAAR TRANSFORM IN SIGNAL ANALYSIS

The Haar transform stands for the simplest algorithm enabling signal or image compression [14].

Let us have a signal $\{x(n)\}_{n=1}^{N}$. Each pair of its subsequent values $\{x(n), x(n+1)\}$ for $n = 1, 3, \cdots, N$ can then be decomposed into two values

$$\begin{pmatrix} X_n \\ X_{n+1} \end{pmatrix} = \mathbf{T} \begin{pmatrix} x_n \\ x_{n+1} \end{pmatrix} \quad (1)$$

using orthogonal decomposition matrix

$$\mathbf{T} = \frac{1}{\sqrt{2}} \begin{pmatrix} 1 & 1 \\ 1 & -1 \end{pmatrix} \quad (2)$$

Resulting sequence $\{X_1, X_3, \cdots, X_{N-1}\}$ defines the low-pass decomposition values with its length halved in comparison with the original sequence. The complementary high-pass sequence is composed of values $\{X_2, X_4, \cdots, X_N\}$ in the same way.

A similar principle can be applied to the analysis of an image $[g(n,m)]_{N,M}$ taking into account that a one-dimensional signal can be considered as a special case of an image having one column only. The elementary decomposition element is a 2 x 2 matrix

$$\begin{pmatrix} g_{n,m} & g_{n,m+1} \\ g_{n+1,m} & g_{n+1,m+1} \end{pmatrix} \quad (3)$$

where $n = 1, 3, \cdots, N-1$ and $m = 1, 3, \cdots, M-1$. Each such submatrix is decomposed column-wise at first

$$\begin{pmatrix} G1_{n,m} & G1_{n,m+1} \\ G1_{n+1,m} & G1_{n+1,m+1} \end{pmatrix} = \mathbf{T} \begin{pmatrix} g_{n,m} & g_{n,m+1} \\ g_{n+1,m} & g_{n+1,m+1} \end{pmatrix} \quad (4)$$

and then row-wise using relation

$$\begin{pmatrix} G_{n,m} & G_{n,m+1} \\ G_{n+1,m} & G_{n+1,m+1} \end{pmatrix} = \begin{pmatrix} G1_{n,m} & G1_{n,m+1} \\ G1_{n+1,m} & G1_{n+1,m+1} \end{pmatrix} \mathbf{T}^T \quad (5)$$

In this manner, the first level of the decomposition procedure is completed. The resulting matrix elements may be rearranged to define four submatrices. The low/low-pass submatrix is defined hereby

$$\begin{pmatrix} G_{1,1} & G_{1,3} & \cdots & G_{1,M-1} \\ G_{3,1} & G_{3,3} & \cdots & G_{3,M-1} \\ & & \cdots & \\ G_{N-1,1} & G_{N-1,3} & \cdots & G_{N-1,M-1} \end{pmatrix} \quad (6)$$

This matrix having the half number of rows and columns comparing to the original one can be used for the next level of decomposition. The results of the 2-D Haar decomposition of a spinal MR image into the first level are presented in Fig. 2.

In a similar way, it is possible to decompose the body consisting of layers of images. The mathematical principle [14, 15] is based upon the generalization of the previous method

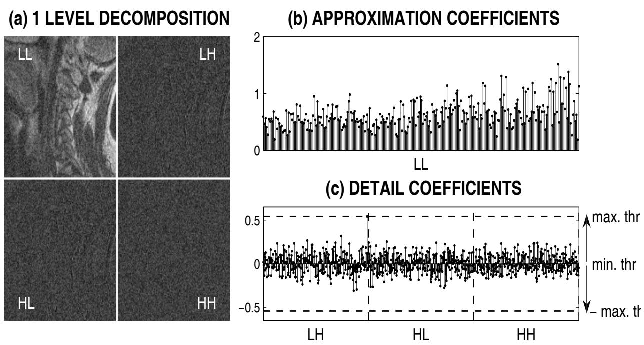

Fig. 2. Haar decomposition of a selected MR image with the additional random presenting **(a)** results of single level image decomposition, **(b)** the approximation decomposition coefficients, and **(c)** the detail decomposition coefficients

adding another axis in the layer direction. In other words, pixels of the outcome of 2-D transform of all image layers, which have the corresponding x,y-location, are treated as 1-D signals. The 3-D decomposition of a spinal MR image volume using the Haar decomposition matrix is shown in Fig. 3. Further possibilities include application of complex wavelet functions [16].

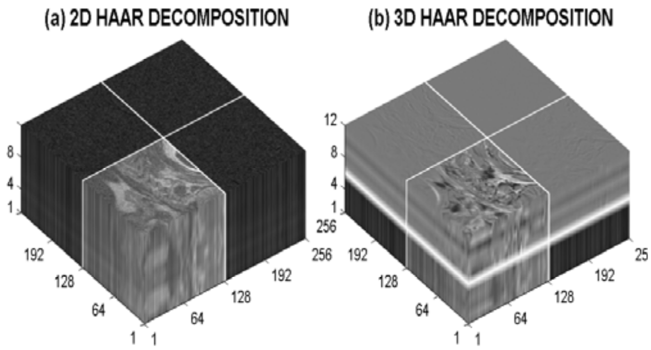

Fig. 3. Decomposition of the set of MR images presenting **(a)** 2-D (slice-by-slice) Haar wavelet decomposition **(b)** 3-D (volumetric) Haar wavelet decomposition

3. OPTIMAL THRESHOLD SELECTION FOR IMAGE DE-NOISING

Image de-nosing can be achieved by appropriate thresholding of wavelet coefficients. In the case of soft-thresholding it is possible to evaluate new coefficients $\overline{c}(k)$ using original coefficients $c(k)$ for a chosen threshold value δ by relation

$$\overline{c}(k) = \begin{cases} \text{sign } c(k)\ (|c(k)| - \delta) & \text{if } |c(k)| > \delta \\ 0 & \text{if } |c(k)| \leq \delta \end{cases} \quad (7)$$

This approach can be exploited for both signals and images using different methods of threshold level estimation. Fig. 4(a) presents the results of a selected numerical experiment of a single layer de-noising showing the dependence of the mean square error (MSE) on the threshold limit ranging from zero to the maximal value of the absolute detail decomposition coefficients. In this way, the optimal value of threshold level is found for each image layer. In the case of 3-D decomposition, a single threshold value is estimated for the whole volume. Results of the 2-D de-nosing of the selected MR image using global thresholding and the optimal threshold value are presented in Figs 4(b), (c) and (d).

4. MULTIDIMENSIONAL OBJECT DE-NOISING

Signal de-noising procedure applied in two dimensions can further be generalized to three dimensions. The study of the extend to which spatial information can improve the result of image de-noising forms the main part of the following work.

Table 1. MRI DATA SETS SPECIFICATIONS

MRI Set	*Data Type*	*Pixel Spacing [mm]*	*Slice Spacing [mm]*	*Block Size*
1	Spine - Sagittal	0.4687	4	512x512x12
2	Spine - Axial	0.3906	4	512x512x26
3	Cut of Set 1	0.4687	4	256x256x12
4	Cut of Set 2	0.3906	4	256x256x26
5	Brain - Axial	0.4688	1	256x256x12

The research is devoted to the problem of noise rejection in real MR images. Table 1 summarizes specifications of MR data sets used in this study presenting different biomedical structures. Fig. 1 shows parts of the set number 3 composed of 12 layers with resolution of 256 x 256 pixels.

Fig. 5 shows the results achieved for selected sets of MR images. The additional random noise was rejected using both 2-D and 3-D Haar decomposition and thresholding of the resulting coefficients.

Numerical results are summarized in Table 2 for five selected MR sets. The mean square error between the original image volume and the de-noised one is normalised to the number of pixels in each image set. For each of the five sets

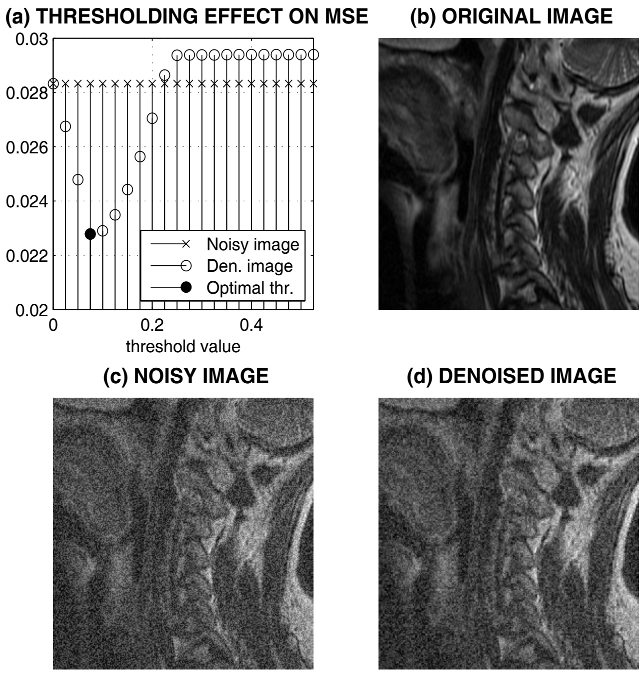

Fig. 4. Processing of the spinal MR image (number 3) presenting **(a)** the effect of threshold selection on the mean square error (MSE) value, **(b)** original image, **(c)** image with additional random noise, and **(d)** de-noised image using the optimal threshold value

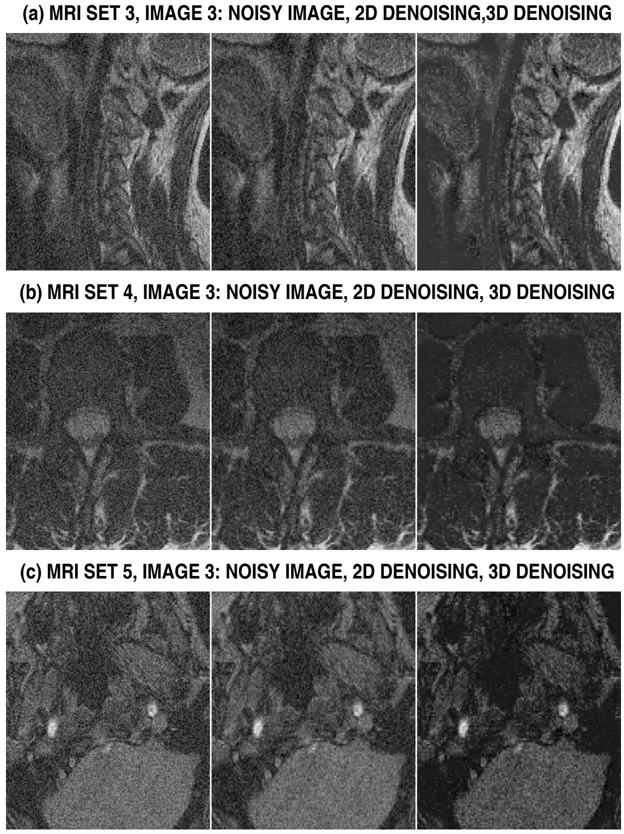

Fig. 5. MR image de-noising by thresholding the 2D and 3D Haar coefficients for **(a)** image number 3 of MRI set 3 (sagittal spine), **(c)** image number 3 of MRI set 4 (axial spine), and **(c)** image number 3 of MRI set 5 (axial brain)

of data, we carried out ten 2-D and ten 3-D de-noising experiments, each time with a different random noise component. Table 2 displays the average MSE, its variance and its percentage improvement attained by de-noising. Both numerical results and their visualization presented in Fig. 5 verify that the 3-D approach to image processing can highly improve results achieved by the de-noising of individual layers.

Another set of numerical experiments have been done with a specific noise component related to the random noise restricted to the higher spectral components in the frequency domain only. Accomplishing the same set of experiments with this high frequency band noise, much better results were achieved for both de-noising methods. The overall average improvement was 74.2% for the 2-D de-noising and 87.2% for the 3-D de-noising. In this case, the advantages of the volumetric approach were not revealed in the full scale.

However, in the case of random noise, the layer-by-layer technique proves insufficient in comparison with the volumetric one. The percentage decrease of the random noise components summarised in Table 2 points out the substantial effect of the 3-D approach. While the overall average improvement

Table 2. COMPARISON OF THE DE-NOISING RESULTS FOR THE 2-D AND 3-D HAAR TRANSFORM

Method / Measure		*MRI Set*				
		1	*2*	*3*	*4*	*5*
2D	*MSE [E-02]*	2.69	2.27	1.81	1.77	1.97
	Variance [E-07]	8.25	3.39	14.9	2.68	13.0
	Improvement [%]	17.9	24.0	26.8	33.4	24.9
3D	*MSE [E-02]*	1.56	0.91	1.14	0.72	0.62
	Variance [E-07]	13.8	1.10	5.40	0.71	1.91
	Improvement [%]	52.5	69.6	53.9	73.0	76.2

was 25.5% for the single layer processing, it was possible to achieve the improvement of 65.0% by the 3-D decomposition and de-noising approach.

5. CONCLUSION

It is possible to summarize that the 3-D image de-noising can significantly improve results achieved in the case of processing of individual images. The results presented in Table 2 summarize numerical experiments for real MR biomedical bodies using the Haar volumeric decomposition enabling also very simple reconstruction of the three-dimensional body.

Further studies will be devoted to the application of specific wavelet functions for volumetric enhancement of biomedical structures. The purpose of such a study is in the detection of image components and in visualization of general slices of the 3-D structures.

6. REFERENCES

[1] D. E. Newland, *An Introduction to Random Vibrations, Spectral and Wavelet Analysis*, Longman Scientific & Technical, Essex, U.K., third edition, 1994.

[2] Saeed Vaseghi, *Advanced Digital Signal Processing and Noise Reduction*, John Wiley & Sons, West Sussex, U.K., third edition, 2006.

[3] N. Kingsbury, "Complex Wavelets for Shift Invariant Analysis and Filtering of Signals," *Journal of Applied and Computational Harmonic Analysis*, vol. 10, no. 3, pp. 234–253, May 2001.

[4] S. Li and J. Shawe-Taylor, "Comparison and Fusion of Multiresolution Features for Texture Classification," *Pattern Recogn. Lett.*, vol. 25, 2004.

[5] M. Weeks and M. A. Bayoumi, "Three-Dimensional Discrete Wavelet Transform Architectures," *IEEE Transactions on Signal Processing*, vol. 50, no. 8, pp. 2050 – 2063, 2002.

[6] J. Ptáček, I. Šindelářová, A. Procházka, and J. Smith, "Wavelet Transforms In Signal And Image Resolution Enhancement," in *International Conference Algoritmy 2002, Podbanske*. 2002, STU.

[7] A. Procházka and J. Ptáček, "Wavelet Transform Application in Biomedical Image Recovery and Enhancement," in *The 8th Multi-Conference Systemics, Cybernetics and Informatic, Orlando, USA*. 2004, vol. 6, pp. 82–87, IEEE.

[8] Xiaohui Yuan and G. Chi-Fishman, "Volumetric Tongue Reconstruction by Fusing Bidirectional MR Images," in *3rd IEEE International Symposium on Biomedical Imaging: Macro to Nano*. 2006, pp. 1352 – 1355, IEEE.

[9] V. Thirumalai and R. Kanhirodan, "Wavelet Transform Codec for Fast Retrieval of Slices of 3D Objects," in *Proceedings of the IEEE Instrumentation and Measurement Technology Conference, IMTC 2005*. 2005, vol. 2, pp. 1251 – 1254, IEEE.

[10] G. Menegaz and L. Grewe and J. P. Thiran, "Multirate Coding of 3D Medical Data," in *Proceedings of the 2000 International Conference on Image Processing*. 2000, vol. 3, pp. 656 – 659, IEEE.

[11] J. Wang and H. K. Huang, "Medical Image Compression by Using Three-Dimensional Wavelet Transform," *IEEE Transactions on Medical Imaging*, vol. 15, no. 4, pp. 547 – 554, 1996.

[12] M. Breakspear, M. Brammer, E. Bullmore, P. Das, and L. Williams, "Spatiotemporal Wavelet Resampling for Functional Neuroimaging Data," *Human Brain Mapping*, vol. 23, no. 1, pp. 1–25, 2004.

[13] E. Bullmore, J. Fadili, V. Maxim, L. Sendur, J. Suckling B. Whitcher, M. Brammer, and M. Breakspear, "Wavelets and Functional Magnetic Resonance Imaging of the Human Brain," *NeuroImage*, vol. 23, no. Sup 1, pp. 234–249, 2004.

[14] D. Montgomery and F. Murtagh and A. Amira, "A Wavelet Based 3D Image Compression System," in *Proceedings of the Seventh International Symposium on Signal Processing and Its Applications*. 2003, vol. 1, pp. 65 – 68, IEEE.

[15] C. Zhang and H. X. Zheng and D. B. Ge, "3-D Wavelet-Based Multiresolution Analysis," in *Proceedings of the 5th International Symposium on Antennas, Propagation and EM Theory*. 2000, pp. 301 – 304, IEEE.

[16] N. Kingsbury and A. Zymnis and A. Pena, "DT-MRI Data Visualisation Using the Dual Tree Complex Wavelet Transform," in *3rd IEEE International Symposium on Biomedical Imaging: Macro to Nano*. 2004, pp. 328 – 331, IEEE.